Romanian Reports in Physics **70**, 201 (2018)

FISSION TIMES AND PAIRING PROPERTIES

M. MIREA[1,2,*], A. SANDULESCU[1,3,4]

[1]Department of Theoretical Physics, Horia Hulubei National Institute for Physics and Nuclear Engineering, Atomistilor 407, RO-077125, POB-MG6, Măgurele-Bucharest, Romania
[2]Academy of Romanian Scientists, Splaiul Independentei 54, RO-050094, Bucharest, Romania
[3]Academia Romana, Calea Victoriei 125, Bucharest, Romania
[4]Geodynamic Institute of the Romanian Academy, 19-21 Jean Louis Calderon, RO-020032, Bucharest 37, Romania
[*]Corresponding author, Email: mirea@ifin.nipne.ro

Received September 1, 2017

Abstract. The dissipated energy is calculated for different values of the tunneling velocity by solving the time-dependent pairing equations. Two models are used for the pairing interaction: a constant value of the pairing interaction and the density dependent delta interaction. The time-dependent pairing equations supply an average value of the dissipated energy at scission. This average value is compared with experimental data. An average tunneling velocity is deduced by selecting the value that gives the best agreement between experimental and theoretical dissipation energies. The tunneling velocity is strongly model dependent, giving much lower values for the formalism that involves state-dependent pairing interactions than that characterized by the constant pairing. The investigation is made for the fission of ^{232}Th, along a fission trajectory that connects the ground state of the parent nucleus to the scission configuration. This fission trajectory is obtained from the least action principle. The rearrangement of the single particle level scheme is supplied by the Woods-Saxon two-center shell model.

Key words: ^{232}Th fission, energy dissipation, pairing models.

1. INTRODUCTION

Due to the viscosity, a part of the collective velocity available in a fission process is transferred as a heat into the intrinsic degrees of freedom [1]. The amount of dissipated energy can be experimentally evaluated by measuring the odd-even effect in the isotopic distributions of fragments [2–5], or the energy released by neutron and gamma-emissions [6]. The dissipated energy increases with the deformation velocity [7]. It was also emphasized that a competitive role in the total excitation energy is played by the deformations of the fragments at scission [8]. As mentioned in Ref. [9], the dissipation effects are better evidenced experimentally at excitation energies lower than 12 MeV. Therefore, a dependence between the scission time and the dissipated energy should be emphasized in this energy domain.

Recent self-consistent calculations emphasized the fact that the fission is an extremely slow process. As discussed in Ref. [10], tunneling velocities of the order of $6{\times}10^4$ up to $2{\times}10^5$ fm/fs can be obtained from scission times [11]. In general, it is accepted that the scission time is of the order of 10^{-21} s. If the elongation is modified with about 3 fm between the top of the outer fission barrier and the scission point, tunneling velocities of 3×10^6 fm/fs can be postulated for this accepted value of the scission time. So the values obtained in Ref. [11] seems to be very small. But, values of the tunneling velocities compatible with the accepted scission time can be extracted from other self consistent investigations of the scission process [12–15]. It should be noted, that in Ref. [10] a good agreement between experimental and theoretical half-lives calculations was obtained for a tunneling mean velocity of 1×10^5 fm/fs. In this work, average tunneling velocities are extracted from the dissipated energy in the fission fragments. The dissipation energy is calculated dynamically by solving the time-dependent pairing equations. The pairing is taken into account within two different formalisms. One of them considers a constant pairing, while the other one, a state dependent pairing interaction. By comparing the dissipated energy with reasonable values that can be obtained experimentally, it is possible to predict tunneling velocities.

2. MODEL

The way to calculate the dissipation energy at scission and the main features of the two pairing mechanisms involved in this work are underlined.

2.1. DISSIPATION

The dissipation is one way to speak about the flow of energy from collective degrees of freedom into intrinsic ones. When the system deforms and arrives in a new configuration, the probabilities of occupation of different intrinsic states should vary in order to reach the stationary values appropriate to the new deformation. But, if the variation of the nuclear deformation is made rapidly, the system has no time enough to rearrange themself. So, a surplus of energy is accumulated in the microscopic degrees of freedom leading to dissipation. It is possible to evaluate the dissipated energy in superfluid systems by solving the time-dependent pairing equations [16–20]:

$$i\hbar\dot{\rho}_k = \kappa_k\Delta_k^* - \kappa_k^*\Delta_k, \tag{1}$$

$$i\hbar\dot{\kappa}_k = (2\rho_k - 1)\Delta_k + 2\kappa_k(\epsilon_k - \lambda) - 2G_{kk}\rho_k\kappa_k. \tag{2}$$

Here, the gap pairing parameter is defined as

$$\Delta_k = \sum_{k'} \kappa_{k'} G_{kk'} \tag{3}$$

and $\rho_k =| v_k |^2$ are the single particle densities while $\kappa_k = u_k v_k$ denote the pairing moment components. As usual, u_k and v_k denote vacancy and occupation amplitudes of the Bogoliubov wave functions, respectively.

The total energy of the nuclear system is

$$E = 2\sum_k \rho_k \epsilon_k - \sum_k \kappa_k \sum_{k'} \kappa^*_{k'} G_{kk'} = \sum_k \rho_k^2 \tag{4}$$

The lower energy state at the same deformation E_0 is obtained by replacing in the previous formula the dynamical parameter ρ_k and κ_k with the stationary values given by the solutions of the stationary BCS equations. The difference $E^* = E - E_0$ represents an estimation of the mean dissipation energy.

2.2. CONSTANT PAIRING INTERACTION

We use two formalisms to deduce the pairing strengths. The first one considers that the pairing interaction is constant in the active pairing level space. Our pairing active level space consists of 28 levels above and below the Fermi level.

For constant pairing interaction G, we used the formula [21, 22]

$$\frac{1}{G} = \tilde{g}(\tilde{\lambda}) \ln\left(\frac{2\Omega}{\tilde{\Delta}}\right) \tag{5}$$

where $\tilde{\Delta} = 12/A^{1/2}$ MeV is smoothed pairing gap parameter that is a good approximation throughout the periodic table. An average level density at Fermi energy is given by $\tilde{g}(\tilde{\lambda})$ that can be calculated using the Strutinsky average procedure. Ω is an energy related to the pairing active level space taken into consideration.

2.3. STATE DEPENDENT PAIRING

In the pairing density-dependent delta interaction approach, the residual interaction is mainly coming from the surface region of the nuclei. The pairing strength is [23–27]:

$$V_p(\vec{r}) = -V_0\left[1 - \beta\left(\frac{\rho(\vec{r})}{\rho_0}\right)^{\gamma}\right], \tag{6}$$

where the parameters are usually $\beta = 1$ and $\gamma = 1$. We denoted with ρ the local density in the point $\vec{r}$ and with $\rho_0 = 0.16$ fm^{-3} the saturation density. The pairing interactions between two single particle states labeled with i and j is defined as

$$G_{ij} = -\int V_p(\vec{r}) \mid \varphi_i(\vec{r}) \mid^2 \mid \varphi_j(\vec{r}) \mid^2 d\vec{r}, \tag{7}$$

where φ_i and φ_j are the single particle wave functions. For ^{232}Th, the parameter V_0 of the interaction was adjusted to be 1808 MeV fm^{-3} and 1688 MeV fm^{-3} for proton and neutron, respectively. Similar values of the interactions were obtained for the α-decay of superheavy elements [28]. Within these parameters, the pairing gap for proton is Δ=0.9 MeV and that for neutron is Δ =0.7 MeV. A number of 60 single particle levels were selected for the active level pairing space.

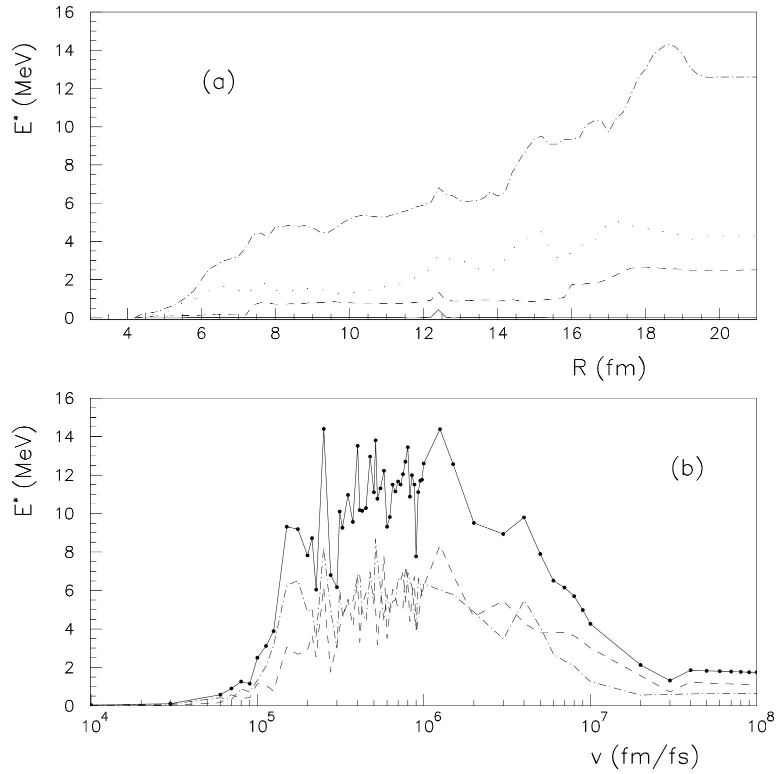

Fig. 1 – Constant pairing interaction. (a) Dissipated energy as function of the internuclear distance R for four tunneling velocities. Full line $dR/dt = 1 \times 10^4$ fm/fs, dashed line $dR/dt = 1 \times 10^5$ fm/fs, dot-dashed line $dR/dt = 1 \times 10^6$ fm/fs, and dotted line $dR/dt = 1 \times 10^7$ fm/fs. (b) Dissipated energy at scission as function of the tunneling velocity $v = dR/dt$. Dot-dashed line neutron dissipated energy, dashed line proton dissipated energy and full line total dissipated energy.

3. RESULTS AND CONCLUSIONS

The fission of ^{232}Th is investigated. A fission trajectory is determined numerically as explained in Ref. [10] where the inertia for the same nucleus is investigated. The main generalized coordinate in our model is the elongation (or the internuclear distance) R defined as the distance between the centers of the two nascent fragments.

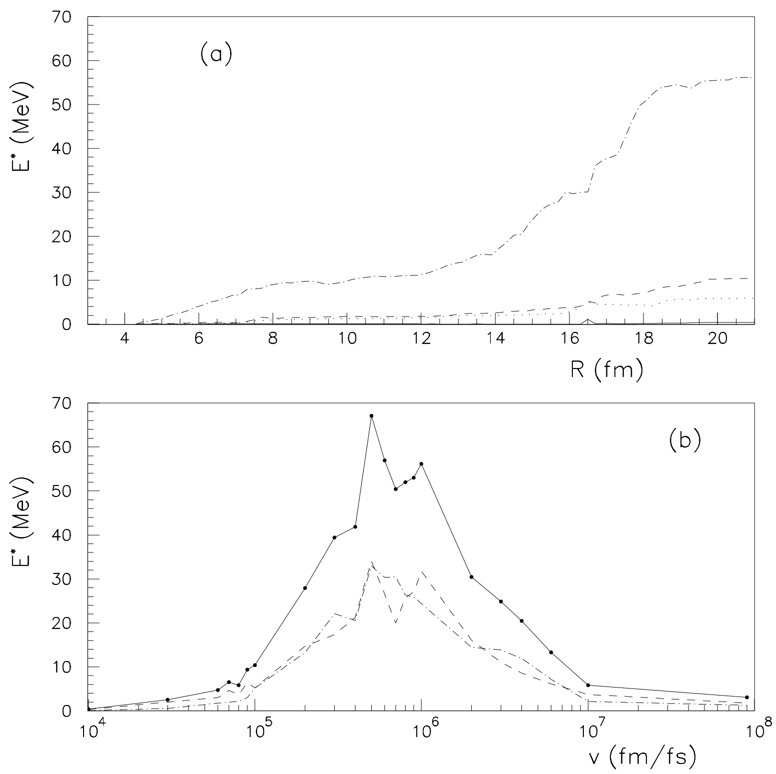

Fig. 2 – Same as in Fig. 1 for the state-dependent pairing interaction.

The single particle levels were calculated within the Woods-Saxon two center shell model [29]. This model is able to describe the passage from one nucleus into two separated bodies in a very accurately way, being useful to characterize scission configurations [30–34]. Even more, this precision also holds true for very large mass-asymmetries, as obtained in the case of alpha or cluster decay [35–38]. In our model, the ground state of ^{224}Th is deformed, the elongation $R \approx$4 fm. The scission point is located at $R \approx$19 fm. Details about these calculations can be found in Ref. [10]. The time-dependent pairing equation were solved beginning from the ground state up to the scission configuration spanning an interval of tunneling velocities $v = dR/dt$ comprised between 1×10^4 and 1×10^8 fm/fs. The variation of the dissipated energies are plotted in panels (a) of Figs. 1 and 2 for the two types of pairing strengths analyzed. First of all, it can be noticed that the dissipated energy increases especially in the region of the outer fission barrier, between R=14 and R=18 fm. This increase of the dissipated energy in the region of the second barrier is more pronounced in the case of state dependent pairing. As expected, in both formalisms the dissipated energy remains unchanged after the scission point. The dissipated energy for the 1×10^4 fm/fs tunneling velocity is negligible. That is, for a very slow deformation of the nuclear system, the nuclear fission process behaves adiabatically. For larger nuclear velocities of the order of 1×10^6 fm/fs, the dissipated energy becomes very large. That is, the nuclear systems proceeds through diabatic states. For tunneling velocities larger than 1×10^7 fm/fs, the final dissipated energy decreases and arrives on a plateau. This happens because we reached the limit of validity of our model. For these large velocities, the passage from the ground state to the scission point is too rapid, the occupation probabilities cannot be modified and the system arrives at scission with occupation probabilities close to the initial ones. An average nucleon velocity of 8×10^7 fm/fs can be associated to the Fermi energy of the nucleons, that is roughly 40 MeV. To allow a rearrangement of the nuclear state, the internuclear velocity should be much smaller than the velocity of the nucleons inside the nucleus. For both pairing mechanisms, the dissipated energy have a maximal value around a velocity of 1×10^6 fm/fs. The striking difference between the two models is the fact that the dissipated energy amounts up to 70 MeV in the case of the state-dependent pairing mechanism.

Table 1

The time for the descent of the barrier for two dissipation energies E^*. The second column is the time T_c for constant pairing and the third column is the time T_d for state-dependent pairing.

E^* (MeV)	T_c (s)	T_d (s)
6	2×10^{-20}	4×10^{-20}
12	0.75×10^{-21}-2×10^{-21}	2.5×10^{-21}

The cold fission is a process in which the dissipated energy is so low that no neutrons can be emitted. So, a dissipated energy of 6 MeV can be considered as an upper value for cold fission processes. From the panels (b) of Figs. 1 and 2, the corresponding velocities for this excitation energy can be deduced as 1.3×10^5 and 7×10^4 fm/fs, respectively. The tunneling velocity is much lower for the state-dependent pairing. In fission, the intrinsic excitation energies at scission are expected to be around 10 MeV for some parent nuclei [39]. Considering that in thermal fission a mean dissipation of 12 MeV is a reasonable value, the corresponding velocities $[4\times10^6 - 1.5 \times 10^6]$ and 1.2×10^6 fm/fs can be estimated for constant pairing and state-dependent pairing interactions, respectively. By considering a modification of the elongation of about 3 fm between the top of the external barrier and the scission point, it is possible to evaluate the time for the descent of the barrier. These times are tabulated in Table 1 for the two investigated energies. We conclude that the tunneling times in fission are strongly model dependent. A realistic pairing interaction produce a fission time considerably longer than a constant interaction. The fission process could be very fast or very slow in superfluid systems to reproduce the same value of an observable, depending on the behavior of the pairing interaction.

Acknowledgements. This work was supported by the grants of Ministry of Research and Innovation, CNCS-UEFISCDI, project numbers PN-III-P4-ID-PCE-2016-0092, within PNCDI III.

REFERENCES

1. R.W. Hasse, Rep. Prog. Phys. **41**, 1027 (1978).
2. K.-H. Schmidt, B. Jurado, C. Amouroux, and C. Schmitt, Nucl. Data Sheets **131**, 107 (2017).
3. B. Jurado and K.H. Schmidt, J. Phys. G **42**, 055101 (2015).
4. C. Giubega, I. Visan, and A. Tudora, Rom. Rep. Phys. **68**, 1024 (2016).
5. A. Tudora, F.-J. Hambsch, G. Giubega, and I. Visan, Rom. Rep. Phys. **68**, 571 (2016).
6. R. Capote *et al.*, Nucl. Data Sheets **131**, 1 (2016).
7. A. Sandulescu and H. Scutaru, Ann. Phys. **173**, 277 (1987).
8. M. Montoya and V. Collin, Rev. Mex. Fis. **63**, 151 (2017).
9. P. Armbruster, Rep. Prog. Phys. **62**, 465 (1999).
10. M. Mirea, J. Phys. G **43**, 105103 (2016).
11. A. Bulgac, P. Magierski, K.J. Roche, and I. Sfetcu, Phys. Rev. Lett. **116**, 122504 (2016).
12. G. Scamps, C. Simenel, and D. Lacroix, Phys. Rev. C **92**, 011602(R) (2015).
13. C. Simenel and A.S. Umar, Phys. Rev. C **89**, 031601(R) (2014).
14. P. Goddard, P. Stevenson, and A. Rios, Phys. Rev. C **92**, 054610 (2015).
15. P. Goddard, P. Stevenson, and A. Rios, Phys. Rev. C **93**, 014620 (2016).
16. S.E. Koonin and J.R. Nix, Phys. Rev. C **13**, 209 (1976).
17. J. Blocki and H. Flocard, Nucl. Phys. **A273**, 45 (1976).
18. M. Mirea, Phys. Lett. B **680**, 316 (2009).
19. M. Mirea, Phys. Rev. C **83**, 054608 (2011).
20. M. Mirea, Phys. Lett. B **717**, 252 (2012).
21. M. Brack, J. Damgaard, A.S. Jensen, H.C. Pauli, V.M. Strutinsky, and C.Y. Wong, Rev. Mod. Phys. **44**, 320 (1972).
22. K. Pomorski and F. Ivanyuk, Int. J. Mod. Phys. E **18**, 900 (2009).
23. R.R. Chasman, Phys. Rev. C **14**, 1935 (1976).
24. J. Dobaczewski, W. Nazarewicz, T.R. Werner, J.F. Berger, C.R. Chinn, and J. Decharge, Phys. Rev. C **53**, 2809 (1996).
25. M. Bender, K. Rutz, P.-G. Reinhard, and J.A. Maruhn, Eur. Phys. J. A **8**, 59 (2000).
26. S. Yoshida and H. Sagawa, Phys. Rev. C **77**, 054308 (2008).
27. N. Tajima, P. Bonche, H. Flocard, P.-H. Heenen, and M.S. Weiss, Nucl. Phys. A **551**, 434 (1993).
28. M. Mirea, Eur. Phys. J. A **51**, 36 (2015).
29. M. Mirea, Phys. Rev. C **78**, 044618 (2008).
30. M. Mirea, D.S. Delion, and A. Sandulescu, Proc. Romanian Acad. A **18**, 50 (2017).
31. M. Mirea, Phys. Rev. C **89**, 034623 (2014).
32. A. Sandulescu and M. Mirea, Eur. Phys. J. A **50**, 110 (2014).
33. D. Aranghel and A Sandulescu, Rom. Rep. Phys. **68**, 160 (2016).

34. D. Aranghel and A. Sandulescu, Rom. J. Phys. **60**, 147 (2015).
35. M. Mirea, Rom. J. Phys. **60**, 156 (2015).
36. M. Mirea and A. Sandulescu, Proc. Romanian Acad. A, in press.
37. M. Mirea, R. Budaca, and A. Sandulescu, Ann. Phys. (N.Y.) **380**, 157 (2017).
38. A. Sandulescu, M. Mirea and D.S. Delion, EPL **101**, 62001 (2013).
39. K.H. Schmidt and B. Jurado, Phys. Rev. C **83**, 061601(R) (2011).